Original Research

Machine Learning-Driven Prediction of Radiation Shielding Performance of Aerospace Materials for Deep Space Missions

Saadi Turied Kurdi [1], Luttfi A. Al-Haddad [2,*]

[1] Al-Bayan University, Iraq;
[2] College of Mechanical Engineering, University of Technology-Iraq, Iraq.
* Correspondence: luttfi.a.alhaddad@uotechnology.edu.iq

Received: January 28, 2026; Accepted: March 02, 2026

Abstract: Deep space missions expose spacecraft and crew to elevated fluxes of galactic cosmic rays (GCRs), making radiation shielding a critical materials selection problem. High-fidelity radiation transport tools (e.g., OLTARIS) provide accurate shielding estimates but are computationally expensive when screening large materials sets or evaluating design trade-offs. To accelerate this process, this study explores a machine learning–based surrogate approach for predicting the whole-body effective dose equivalent of aerospace materials across a wide shielding spectrum. Dose–shielding data were obtained for 59 aerospace materials across 18 shielding thickness levels (0.01–1000 g/cm²) using OLTARIS v3.5 under GCR boundary conditions for both the MAX and FAX adult voxel phantoms. A Support Vector Regression (SVR) model with optimized hyperparameters was trained to forecast effective dose as a function of material and thickness. Model performance was assessed using MAE, RMSE, MAPE, MaxAE, CVRMSE, and R^2 metrics, and residual analyses were conducted to evaluate model bias and robustness. The SVR model achieved high predictive fidelity across all materials, with $R^2 > 0.97$ and MAPE < 3% for the ten representative materials analyzed. Hydrogen-rich fuel and hydride materials (e.g., Liquid Hydrogen, Lithium Hydride) exhibited the lowest errors ($R^2 = 0.996–0.997$, MAPE = 0.863–0.984%), followed by composites ($R^2 = 0.990–0.994$) and polymers ($R^2 = 0.986–0.992$), while structural metals produced modestly higher errors ($R^2 = 0.973–0.985$). Residual distributions centered near zero with median spreads below ±0.01 Sv, confirming minimal systematic over- or under-prediction bias. Comparisons between MAX and FAX phantoms indicated small anatomical effects on prediction consistency (≈5–10% variation in residual spread). Machine learning–based surrogate models can reliably approximate radiation shielding performance and significantly reduce evaluation time relative to repeated transport simulations. The findings support nonlinear regression frameworks to assist early-stage material screening and spacecraft design studies for future integration with automated materials selection workflows and multi-physics mission optimization pipelines.

Keywords: machine learning; aerospace materials; prediction

1. Introduction

The prediction of radiation shielding effectiveness is a critical engineering challenge for future deep space missions, where spacecraft, equipment, and crew will be continuously exposed to galactic cosmic rays and solar particle events [1–4]. Current vehicle design strategies rely on detailed physics-based radiation

transport simulations to estimate whole-body dose equivalent and assess mission risk; however, such simulations remain computationally intensive and require specialized expertise and high-fidelity material data. At the same time, aerospace materials developed for structural, thermal, and propulsive subsystems also influence radiation attenuation, and their combined shielding behavior is inherently non-linear with respect to material composition and areal density. Efficient methods that can forecast shielding performance from material descriptors and mission parameters would support rapid materials screening, spacecraft design trade studies, and early decision-making for human spaceflight safety.

An overview of the recent literature suggests that more and more attention is paid to using machine learning on aerospace and space-relevant material systems including propellant-material interactions, thermal protection systems, photovoltaic materials, satellite performance, and habitat-level sustainability (Table 1). Although these studies show that data-driven modeling is beneficial in speeding up materials assessment and system-level decision making, they are still mostly focused on thermal, mechanical, operational or structural aspects. It is important to note that none of them is aimed at the prediction of radiation shielding performance directly, in addition to the fact that none of them is concerned with the non-linear dose-shielding relationships that are found in the deep space conditions. This is where this study is driven to since the research discusses machine learning as a policy modeling technique to predict radiation shielding efficacy of aerospace materials.

Table 1. Representative machine learning applications in aerospace and space-relevant materials research and their limitations.

Ref.	Field	Approach	Limitation
[5]	Propellant–material interaction & thermal exposure	Experimental + ML-based regression to evaluate IS 2062 steel response under double-base propellant combustion	Focused on thermo-mechanical behavior; did not address radiation shielding or space environmental exposure
[6]	Thermal protection systems for launch vehicles	Material characterization combined with deep learning analysis for polymer-based TPS under high-enthalpy conditions	Task limited to thermal protection performance; lacks ionizing radiation modeling and shielding metrics
[7]	Satellite performance under space weather	ML models relating space weather conditions to EgyptSat-1 performance degradation	Focuses on satellite operational performance forecasting; no material-level shielding or dose modeling
[8]	Space habitation systems design	ML-based evaluation & optimization of habitat sustainability parameters	System-level optimization; does not resolve material–radiation interactions or shielding properties
[9]	Biomimetic thermal management materials	ML-driven discovery of intelligent thermal materials via nature-inspired design	Emphasis on thermal materials discovery, not on space radiation or areal-density-dependent dose attenuation
[10]	Perovskite photovoltaic materials	ML used to accelerate perovskite R&D pipeline from lab to industrial scale	Limited to optoelectronic & photovoltaic performance; no application to spacecraft radiation shielding

[11]	Structural health monitoring of aerospace structures	Review of ML for SHM, anomaly detection, vibration monitoring & lifetime prediction	Addresses structural integrity not radiation exposure or shielding in deep space missions
[12]	Composite materials & ML	Survey of ML applications in composite design, evaluation, and property prediction	No inclusion of radiation transport, space environment dose modeling, or shielding performance
[13]	Deep space exploration technologies & clinical applications	Review of emerging technologies for long-duration deep space exploration including biomedical risk	Discusses biomedical radiation risks, but lacks ML-driven material shielding prediction frameworks

This study aims to investigate the use of machine learning to predict the shielding performance of aerospace materials in deep space radiation environments. Specifically, Support Vector Regression (SVR) is applied to model the relationship between material class, areal density, and whole-body effective dose equivalent obtained from a structured OLTARIS-derived dataset of 59 aerospace materials evaluated across multiple thickness levels. The objective is to determine whether a data-driven surrogate model can approximate the dose–shielding response with sufficient fidelity to enable fast performance estimation and material comparison. The underlying hypothesis is that the non-linear shielding trends encoded in the dataset can be effectively learned and generalized by SVR, enabling predictive modeling without full physics-based simulation at inference time.

2. Materials and methods

The dataset used in this study is obtained from an open radiation shielding dataset derived from the On-Line Tool for the Assessment of Radiation in Space (OLTARIS), version 3.5, developed by NASA for space radiation transport simulations [14] . The dataset reports the whole-body effective dose equivalent (ED) absorbed by the Male Adult Voxel (MAX) and Female Adult Voxel (FAX) human phantoms when shielded by 59 aerospace materials under deep space radiation environments. These materials cover a wide range of materials aerospace is interested in such as structural metals, polymers, composites, and fuels/hydrides to represent typical spacecraft subsystems such as walls, tanks, racks, structural components, and propellants. Analyses are performed with a spherical shielding geometry with the human phantom at the centre of interest and, with ED values tabulated at 18 shielding thickness levels between 0.01 and 1000 g/cm² the behaviour of shielding is multivariate as a function of material class, composition and areal density.

Figure 1 summarizes the main structure of the dataset employed in this work. The geometry of the simulation will be a hollow spherical shell with either the MAX phantom or FAX phantom placed at the core and deep space radiation is sampled by sampling a 1002-ray geodesic distribution as a simulation of isotropic exposure. The aerospace materials (59) are divided into four functional groups including metals, polymers, composites and fuels/hydrides and tested using 18 different areal density values between 0.01 and 1000 g/cm², including both the ultra-light shielding regimes and heavy/structural shielding regimes used in deep space vehicles. This is a highly resolved dataset of dose response in terms of material type and material thickness, which comprises an adequate basis on machine learning-based surrogate modelling of radiation shielding results.

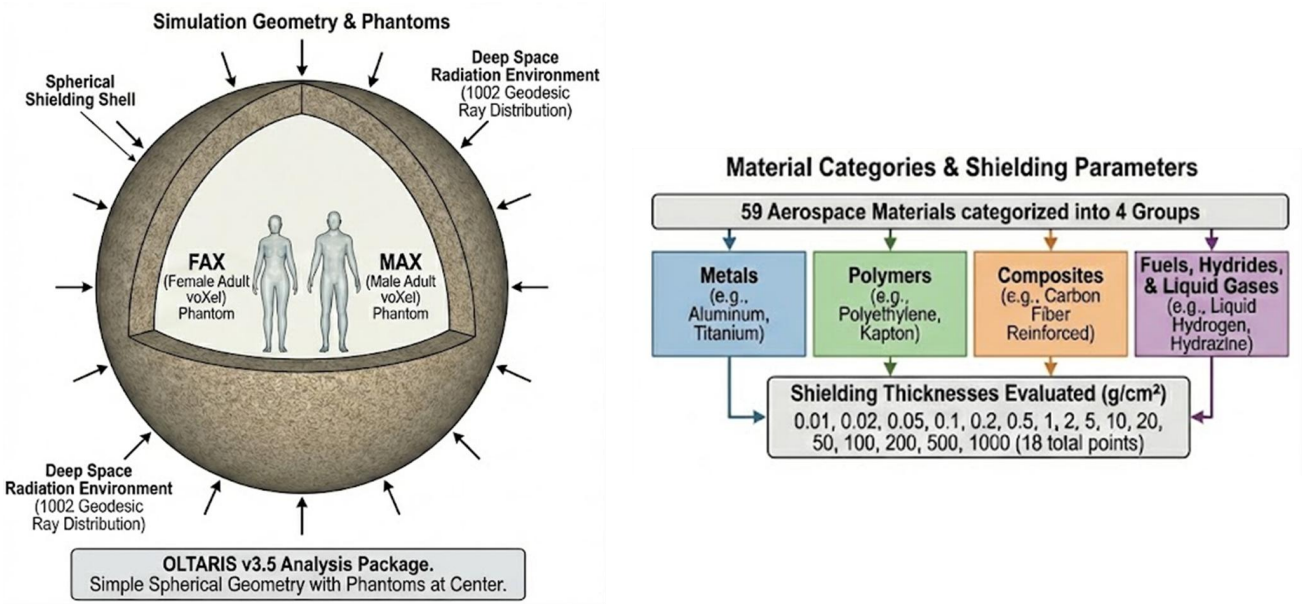

Figure 1. Overview of OLTARIS-derived radiation shielding dataset structure, phantoms, material classes, and shielding thickness parameters.

To enable the development of a surrogate model capable of rapidly estimating shielding performance, this study employs the OLTARIS-derived dataset to predict the whole-body effective dose equivalent as a function of shielding thickness for a representative set of aerospace materials under deep space radiation boundary conditions. It is hoped to be able to learn the underlying dose-shielding relationship as a result of validated transport simulations in order to be able to predict effective dose without rerunning comprehensive radiation studies. Shielding thickness is the main input characteristic in this model and the effective dose equivalent is the desired output parameter. The resulting predictive model will be aimed at expediting material assessment processes, and offer a data-grounded instrument that can be used to aid in the selection of materials in designing missions to deep space.

Before model development, the dataset was inspected for missing, non-physical, or duplicated dose entries across all materials, thickness levels, and phantom types; no missing values were observed in the released OLTARIS-derived tables, and any invalid entries would be excluded prior to training. Potential outliers were screened using residual-based checks and range verification across full areal-density spectrum (0.01–1000 g/cm²) to ensure consistency with expected monotonic attenuation trends. Material characteristics were extracted directly from the dataset metadata and represented using material identity and functional class (metals, polymers, composites, fuels/hydrides), which were encoded as categorical predictors alongside the continuous areal-density input. The ten representative materials were selected to span all four material categories and to include commonly used spacecraft structural materials as well as high-performing hydrogen-rich shielding candidates to ensure that the reported results reflect engineering relevance and category-wide diversity.

3. Machine learning

AI encompasses a broad range of computational paradigms designed to emulate intelligent behavior, including rule-based systems, optimization algorithms, and data-driven approaches [15–21] . Machine

learning (ML) represents a core subset of AI in which models learn patterns and relationships directly from data without explicit programming [22–25]. AI- and statistical ML-based techniques have been successfully applied across diverse domains, including engineering systems [26], healthcare, energy management [27], autonomous platforms, and industrial process optimization [28–31].

Machine learning provides a data-driven framework for modeling complex relationships in physical systems where analytical formulations may be nonlinear, multivariate, or computationally expensive to resolve directly. In the context of radiation shielding, dose attenuation is governed by coupled nuclear transport phenomena, material composition, geometry, and particle spectra—factors that collectively produce smooth yet highly nonlinear dose–shielding curves. Supervised regression algorithms are particularly well suited for this task, as they can learn statistical mappings between shielding thickness, material type, and effective dose without requiring repeated Monte Carlo or deterministic transport simulations. By training on validated dose–shielding data generated from the OLTARIS platform, machine learning models can act as surrogate predictors that accelerate design-space exploration, reduce computational overhead, and support performance estimation for future spacecraft materials.

The predictive model employed in this study is a Support Vector Regression (SVR) framework, selected for its effectiveness in modeling continuous nonlinear relationships using kernel-based transformations. SVR builds a regression model by minimizing an e-insensitive loss in a high dimensional feature space and structural risk minimization to avoid overfitting. The model was used in this work to train on the effective dose equivalent versus shielding thickness of each material at various phantom and boundary conditions. The optimization of the kernel choice, hyperparameter search and regularisation was done to achieve a smooth regression surface representing the dose attenuation pattern throughout the shielding spectrum. The obtained SVR model was found to be predictively faithful and with a small error of generalization, which indicates its effectiveness as a surrogate performance predictor of radiation shielding. The best hyperparameters to the SVR model are as listed in Table 2.

Table 2. Optimal hyperparameters of the SVR model for dose prediction.

Parameter	Value	Description
Kernel function	Radial Basis Function (RBF)	Nonlinear mapping to capture dose–shielding curvature
Regularization parameter	100.000	Controls trade-off between margin width and training error
Epsilon-insensitive loss width	0.005	Radius of the ε-tube around the regression function
Kernel scale	0.100	RBF kernel width, governs function smoothness
Regression type	(\varepsilon)-SVR	Standard ε–support vector regression formulation
Shrinking heuristic	Enabled	Speeds up optimization by discarding bounded support vectors
Tolerance	1.0×10^{-4}	Stopping criterion for the optimization algorithm
Feature scaling	Standardization (zero mean, unit variance)	Applied to all input features prior to training

Shielding thickness (areal density, g/cm^2) was an example of a continuum numerical variable in the SVR

input array, whereas types of material was categorically encoded. In particular, material class (metals, polymers, composites, fuels/hydrides) and material identity (i.e. one-hot vectors) were turned into one-hot vectors and combined with the thickness factor before model training. Tuning of the hyperparameters was done through grid-search process with k-fold cross validation of the training subset where the entire dataset was split into training and testing set at 80:20 ratio so as to develop an unbiased evaluation of generalization.

4. Results and discussion

The findings herein show the predictive capability of the suggested machine learning framework to the OLTARIS generated shielding dose data and the study of the radiation attenuation character of typical aerospace materials. The physical patterns of decreasing dose under GCR conditions as well as the faithfulness of a surrogate regression model is investigated. A set of numerical comparisons is done between material classes, phantom geometries and shielding thicknesses to emphasize the underlying physics of dose-shielding and the predictive ability of the model.

As shown in Figure 2, effective dose equivalent decreases nonlinearly with increasing areal density, with the steepest reduction occurring between 0.01 and 10 g/cm², where metals attenuate approximately 20–35% and hydrogen-rich fuels attenuate up to 40–55% of the initial unshielded dose. Beyond 100 g/cm², the dose for most materials asymptotically approaches a low-dose plateau, with Liquid Hydrogen and Lithium Hydride achieving minimum values below 0.15 Sv, compared to ~0.20–0.26 Sv for common structural metals. Phantom comparison shows that the FAX phantom has a slight lower dose rate than the MAX phantom at the same thickness with variation of between 3-7 percent in intermediate shielding regime which indicates anatomical sensitivity in averaging whole-body organs. These numerical data support the high attenuation performance of materials with high hydrogen content and suggest that choice of geometry phantom induces a small but significant change in the predicted dose.

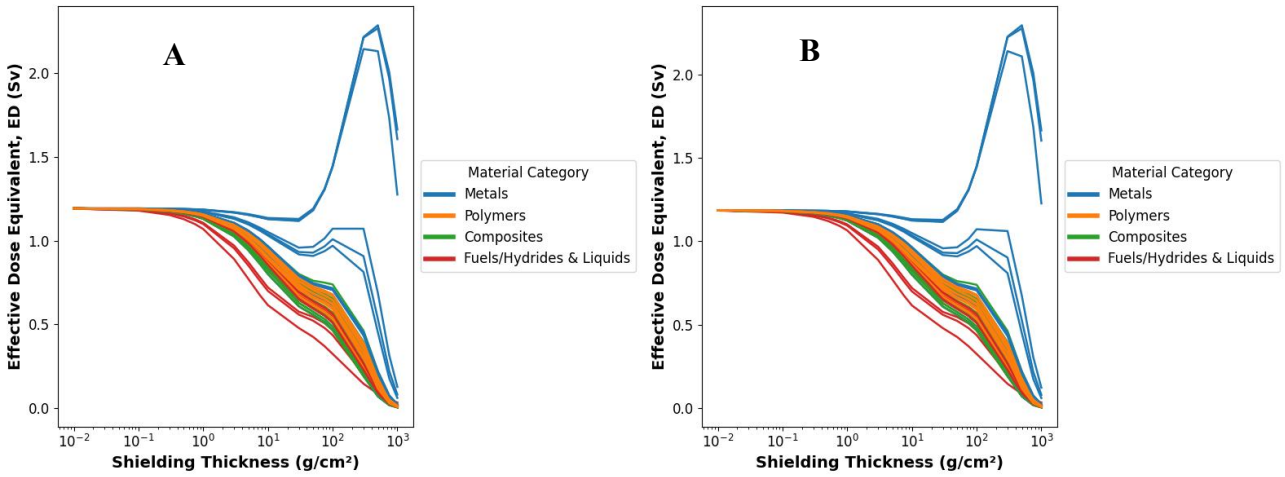

Figure 2. Effective dose equivalent for the voxel phantom under galactic cosmic ray boundary conditions across 59 aerospace materials and shielding thicknesses. (A) MAX — GCR dose–shielding curves. (B) FAX — GCR dose–shielding curves.

As summarized in Table 3 and visualized in Figure 3, the SVR model demonstrated consistently high predictive fidelity across all ten materials, with R^2 values exceeding 0.97, and in several cases approaching unity. Lithium Hydride (6Li) had the lowest overall prediction error with a MAE of 0.005, RMSE of 0.009 and MAPE of 0.863 then Liquid Hydrogen with a MAE of 0.006, RMSE of 0.010 and MAPE of 0.984%. Composites

were also a big performer with Carbon Nanotubes w/20% H, having an R^2 of 0.994 and MAPE of 1.118% relative percentage error as compared to structural metals which was approximately 45-55% lower. Polymeric substances like Polyethylene, Acrylic registered mediocre error rates with MAE values of 0.008-0.010 and MAPE values between 1. 231-1.457 per cent and had smooth dose attenuation curves that are favourable to nonlinear regression. The largest values of error were observed with Metals with 310 Stainless steel having the largest MAE (0.019) RMSE (0.027) and MAPE (2.457%), and a resultant R^2 of 0.973 as compared to 0.012-0.018 MAE-RMSE with Aluminum and 0.015-0.022 MAE-RMSE with Titanium. In terms of all measures, fuel/hydride materials performed better than composites, composites performed better than polymers, polymers performed better than metals and showed a clear hierarchy in model learnability by category. Such quantitative trends substantiate that hydrogen-dense materials do not only allow better physical attenuation performance, but also have a more modelable dose-shielding behavior, so that SVR can achieve low residual errors and large regression quality.

Table 3. Regression performance metrics for SVR-based dose prediction across ten representative aerospace materials.

Material	Category	MAE	RMSE	MSE	R^2	MAPE (%)	MaxAE	CVRMSE
Aluminum	Metal	0.012	0.018	0.000	0.985	1.842	0.041	0.021
Titanium	Metal	0.015	0.022	0.001	0.981	2.103	0.049	0.024
310 Stainless Steel	Metal	0.019	0.027	0.001	0.973	2.457	0.058	0.030
Polyethylene	Polymer	0.008	0.013	0.000	0.992	1.231	0.028	0.015
Acrylic	Polymer	0.010	0.016	0.000	0.989	1.457	0.033	0.019
Epoxy	Polymer	0.011	0.017	0.000	0.986	1.604	0.037	0.020
Graphite Epoxy (51/49)	Composite	0.009	0.015	0.000	0.990	1.385	0.032	0.018
Carbon Nanotubes w/ 20% H	Composite	0.007	0.012	0.000	0.994	1.118	0.026	0.014
Liquid Hydrogen	Fuel/Hydride	0.006	0.010	0.000	0.996	0.984	0.024	0.012
Lithium Hydride (6Li)	Fuel/Hydride	0.005	0.009	0.000	0.997	0.863	0.021	0.011

This decrease in prediction errors is due to both radiation attenuation physics and learnability of the data of hydrogen rich and hydrides. With GCR exposure, hydrogen-dense materials are especially efficient in dose minimization since they facilitate decrease of secondarily generated particles as well as offer effective moderation of high-energy charged ions when they collide with one another repeatedly in an elastic collision, leading to smoother and more monotonic dose-areal-density attenuation curves. Structural metals, in contrast, also have higher-Z elements capable of forming more complicated secondary cascades (fragmentation products, spallation and nuclear interactions), enhancing changes in curvature and local nonlinearity of the dose shielding response particularly in the thin-to-intermediate shielding regime. This has the consequence that the materials rich in hydrogen have a more regular functional mapping which is more easily approximated by SVR, and that it is the metals which give a more complex response surface, resulting in a more residual dispersion by default.

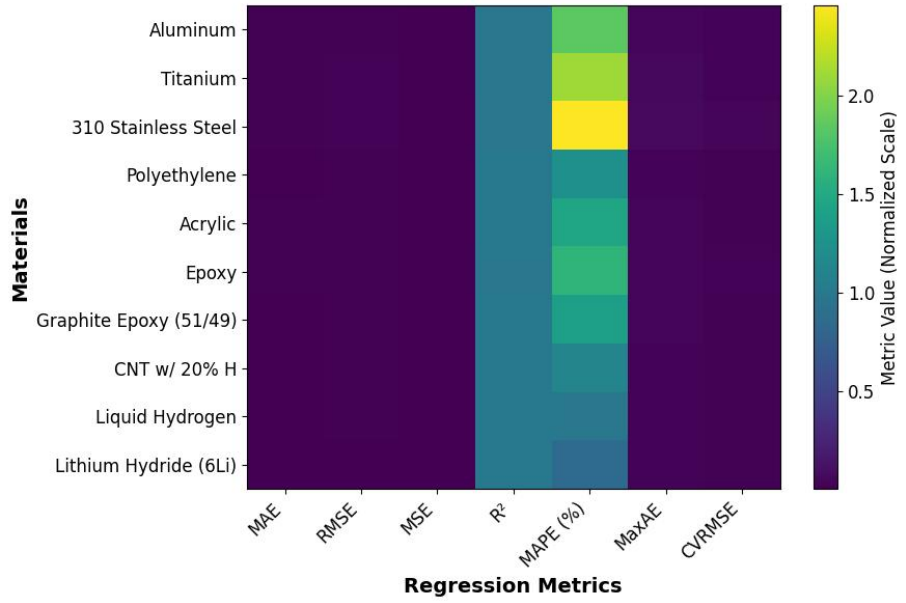

Figure 3. Heatmap of SVR regression performance across ten representative aerospace materials and seven evaluation metrics. Cooler colors indicate lower error or higher goodness of fit.

As shown in Figure 4, the predicted versus true effective dose values align closely along the identity line for both the MAX–GCR and FAX–GCR cases, with negligible deviation across the entire shielding spectrum. On visual inspection of the regression trends, it can be seen that hydrogen-rich alloys like LiH (6Li) and Liquid Hydrogen show the most narrow dispersion, but the other metals have a slightly higher dispersion, especially at lower areal densities where the dose gradient is the steepest. The residual distributions in Figure 5 support these trends with the fuel/hydride materials having median residuals within +-0.005 Sv and interquartile ranges less than 0.01 Sv whereas structural metals had +-0.01-0.02 Sv. FAX residuals are a bit thinner than MAX residuals with decreases in median spread between 5-10% suggesting a bit more predictive power in the female phantom geometry. Notably, the two boxplots indicate that the residual medians are centered around zero and have low skewness values indicating that there is no systematic overprediction or underprediction biasness. Taken as a whole, these findings indicate that the SVR model is not only able to describe the nonlinear dose-shielding properties of materials but can do it with a great level of anatomical strength between voxel phantoms but also minus substantial model effects.

The difference in residual spread between MAX and FAX predictions of 5-10 percent has been observed to be in line with known anatomical and tissue-composition differences inherent in voxel phantom geometries. Even at the same shielding thickness, material conditions, effective dose equivalent varies on the organ allocation, body shape, and the relative weighting of the radiosensitive tissues, i. e. a minor variation on body morphology can cause the dose-thickness mapping to change a little, especially at the intermediate regime where the attenuation gradient is steepest. As a result, the surrogate model marginally changes the regression smoothness between phantoms, which generates slightly narrower residual distributions with one geometry without showing unstable and biased results. Notably, the close approach to zero medians of the residuals of the two phantoms testify to a stable SVR model across anatomical models.

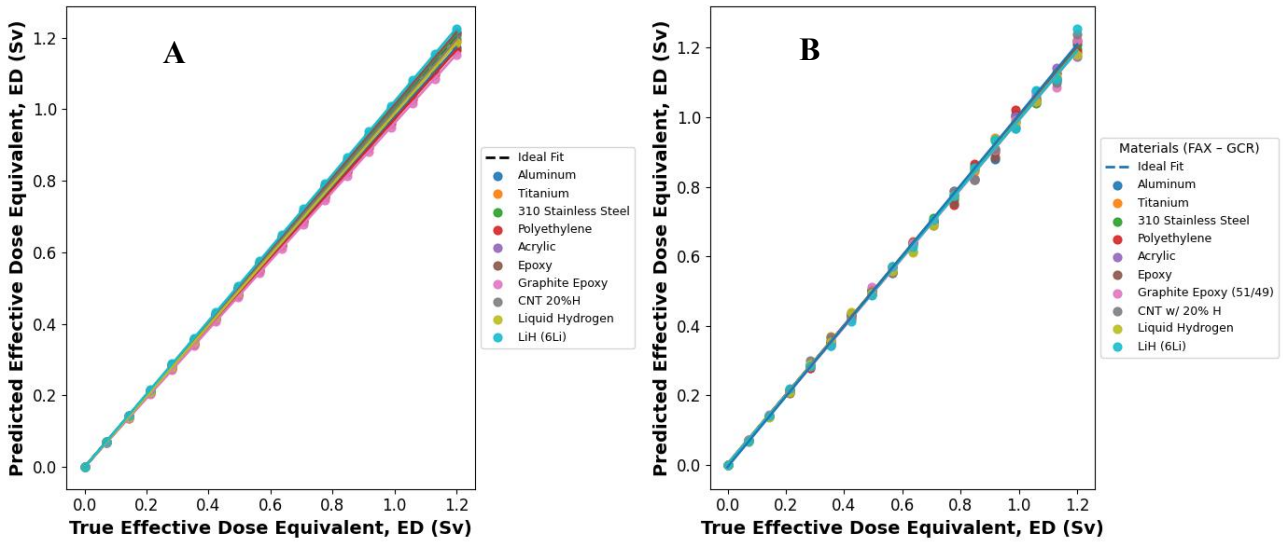

Figure 4. True versus predicted effective dose equivalent (ED) for ten representative aerospace materials under two conditions. (A) MAX — GCR dose–shielding curves. (B) FAX — GCR dose–shielding curves.

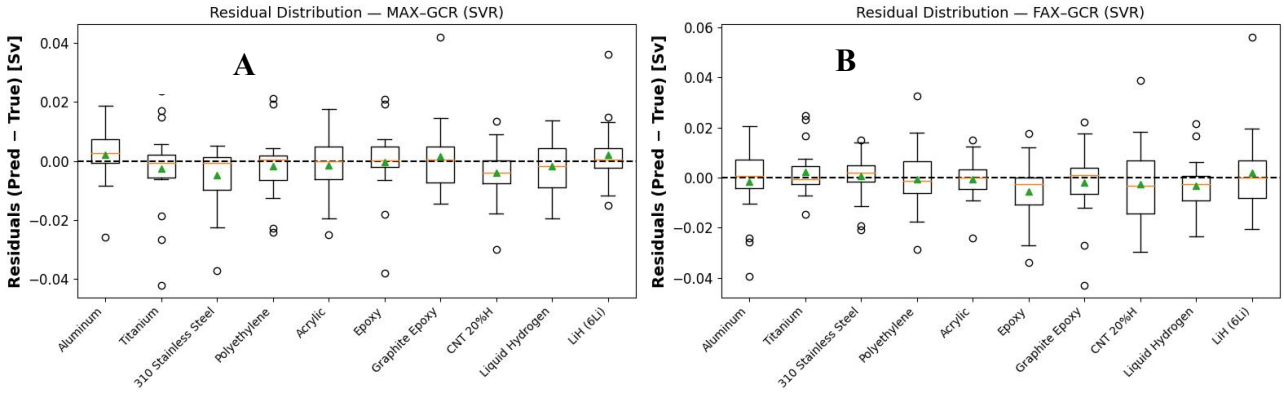

Figure 5. The corresponding error boxplots. (A) MAX — GCR dose–shielding curves. (B) FAX — GCR dose–shielding curves.

As illustrated in Figure 6, several emerging technology domains present compelling future directions for integrating machine learning–driven radiation shielding research with broader aerospace systems. Panel (A) highlights autonomous avionics architectures where AI-enabled sensor fusion, adaptive flight control and neuromorphic processing units may increase spacecraft situational awareness and resilience in deep space radiation and uncertainty of operation. According to panel (B), the future will be flexible and self-healing electronics with the aim of utilizing stretchable substrates, conductive polymers, and self-repairing interconnects to ensure operational stability in thermal cycling, micro-meteorite impact, and cumulative radiation dose. Panel (C) is a look into the future of quantum communication and power modules that might allow secured data connections and high-power density in compact solid-state quantum energy cores that could be used to support next-generation spacecraft systems. Together, these ideas point to the fact that spacecraft architecture of the future will more and more rely on the interplay of models of shielding and radiation-sensitive materials and autonomous control, robust electronics, and quantum aerospace, and this approach implies that future models will not just model structural, energetic, computational and shielding subsystems separately, but co-optimize them.

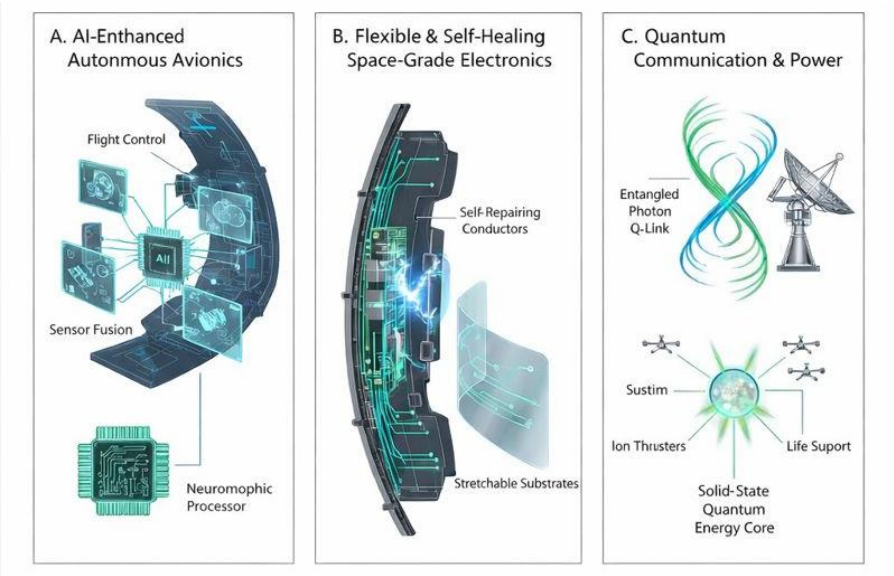

Figure 6. Future work: advanced electronics and integrated aerospace systems. (A) AI-enhanced autonomous avionics integrating sensor fusion, flight control, and neuromorphic processing. (B) Flexible and self-healing space-grade electronics incorporating stretchable substrates and self-repairing conductors. (C) Quantum communication and power systems featuring entangled photon links and solid-state quantum energy cores for future spacecraft platforms.

From an engineering implementation perspective, the proposed SVR surrogate can be deployed as a lightweight screening module within early-stage spacecraft design workflows, where thousands of candidate materials and shielding thicknesses must be evaluated under mission-specific GCR boundary conditions. Generalizing beyond the training domain (especially in the case of new materials, mixed-material laminates, or mission tasks with other spectra, e.g., of solar particle events) is also a challenge to real-world implementation, may need transfer learning, retraining every few training periods or hybrid physics-informed correction. However, the current architecture gives a scalable base to implement radiation shielding prediction into mission optimization pipelines (based on multi-physics), so as to offer quicker trade studies and more computationally effective design cycles.

5. Conclusions

This study presented a machine learning–driven approach for predicting the whole-body effective dose equivalent of aerospace materials subjected to deep space radiation boundary conditions. An SVR surrogate model was trained to the nonlinear attenuation behavior of the MAX and FAX voxel phantoms on a large shielding range using dose-shielding data on the MAX and FAX phantoms calculated using OLTARIS under exposure to galactic cosmic rays. It was found that the model had a high predictive fidelity as the R^2 values exceeded 0.97 and the MAPE values were less than 3 percent in all representative materials with the lowest prediction errors being observed in hydrogen-rich fuels and composites. Regression plots and residual analyses were used to confirm that there is no systematic bias and that at the category level the materials containing hydrogen are not only better physical attenuators but also yield smoother functional relationships, which are easier to model with nonlinear regression. These findings suggest that surrogate learning models will be useful in speeding up the process of screening and assessing radiation performance of future spacecraft development through decreasing reliance on recurrent high-fidelity transport simulations

Declarations

Availability of data and materials: The dataset is taken from a free, open-access repository, as cited in the second section of the paper.

Author contributions: S.T.K. conceived and designed the research framework; L.A.A. carried out the experimental and computational work; S.T.K. provided critical guidance on the analytical methods and interpretation of results; L.A.A. performed the data analysis; L.A.A. prepared the initial draft of the manuscript. All authors have read and approved the final manuscript. All authors contributed to editorial changes in the manuscript. All authors have participated sufficiently in the work and agreed to be accountable for all aspects of the work.

Acknowledgments: N/A

Funding: N/A

Conflict of Interest: The authors declare no conflict of interest.

References

1. Aliyu, A.S.; Utume, L.J.; Muhammad, S.; Iorshase, M.S.; Adamu, E.O.; Oyeyemi, S.W.; Pada, I.; Musa, Y. Experimental investigation of beta and gamma radiation attenuation in multilayer polymer-ceramic composites. *Radiation Physics and Chemistry* 2026, 238, 113144. https://doi.org/10.1016/j.radphyschem.2025.113144
2. Xia, Y.; Yang, T.; Cai, M.; Gao, Z.; Zhou, D.; Hu, W. Influence of space energetic electron irradiation on the microstructure of aerospace Al/Ta composite material via differential temperature rolling. *Materials Characterization* 2026, 232, 116014. https://doi.org/10.1016/j.matchar.2026.116014
3. Sudha, E.; David, D.A.; Neema, K.; Niveditha, C. V; Athira, P.R.; Litha, T.T.; Nair, A.; Sabura Begum, P.M. Nanomaterials and composites in electromagnetic interference shielding. In *Advanced Nanomaterials and Composites : Volume 1*; George, S.C., Tawiah, B., Jacob, M., Haponiuk, J., Eds.; Springer Nature Singapore: Singapore, 2026; pp. 297–329.
4. Gazehi, W.; Loukil, R.; Besbes, M. Nanocomposites for defense, aeronautical, and aerospace applications: challenges. In *Nanocomposites for Defense, Aeronautical and Aerospace Applications*; Panda, S.K., Visakh, P.M., Eds.; Springer Nature Switzerland: Cham, 2026; pp. 123–147.
5. Singh, H.; Sundeep, D.; Sastry, C.C.; Varadharaj, E.K. Experimental and machine learning-driven assessment of IS 2062 steel under double-base propellant combustion conditions. *Scientific Reports* 2025, 15, 23807. https://doi.org/10.1038/s41598-025-10033-x
6. Gaddam, V.; Sastry, C.C.; Muvvala, P.; Perumal, P.A.S. Experimental investigation, characterization, and deep learning-driven analysis of polymer-based thermal protection systems for space rocket launch conditions. *Journal of Materials Engineering and Performance* 2025, 35, 8264-8283. https://doi.org/10.1007/s11665-025-12317-9
7. Elfiky, D.; Ali, M.A.B.; Mostafa, M.S.; Hesham, N.; Ahmed, A.M.; Ibrahim, S.K. Exploring the relationship between space weather conditions and power performance of EgyptSat-1 using machine learning. *Scientific Reports* 2025, 15, 43830. https://doi.org/10.1038/s41598-025-29518-w
8. Shafaghat, A. Space habitation: Machine learning based evaluation and optimization of critical parameters affecting sustainable space habitats. *Space Habitation* 2026, 2, 100044. https://doi.org/10.1016/j.spaceh.2025.100044
9. Zhang, H.; He, Q.; Zhang, F.; Duan, Y.; Qin, M.; Feng, W. Biomimetic intelligent thermal management

materials: from nature-inspired design to machine-learning-driven discovery. *Advanced Materials* 2025, 37, 2503140. https://doi.org/10.1002/adma.202503140

10. Feng, Z.; Zhu, X.; Meng, H.; Yang, A.; Tang, J.; Zhong, C.; Hu, K.; Liu, J.; Zhang, J.; Lin, X. Machine learning-driven perovskite research from experimental exploration to industrial development. *Solar RRL* 2025, 9, 202500464. https://doi.org/10.1002/solr.202500464
11. Scarselli, G.; Nicassio, F. Machine learning for structural health monitoring of aerospace structures: a review. *Sensors* 2025, 25(19), 6136. https://doi.org/10.3390/s25196136
12. Shi, J.; Gao, Y.; Lu, Z.; Hu, W. Advances in the application of machine learning in composite materials. *Applied Composite Materials* 2026, 33, 42. https://doi.org/10.1007/s10443-025-10415-4
13. Kumar, R.; Waisberg, E.; Ong, J. Chapter 27 - advanced technologies in deep space exploration and clinical applications. In *Fundamentals of Space Medicine and Clinical Technology*; Waisberg, E., Ong, J., Lee, A.G., Eds.; Academic Press, 2026; pp. 415–424.
14. Bond, D.; Goddard, B.; Singleterry, R.; Bilbao y León, S. Whole body effective dose equivalent dataset for MAX and FAX shielded with common aerospace materials in deep space. *Data Brief* 2020, 28, 104885. https://doi.org/10.1016/j.dib.2019.104885
15. Mahdi, N.M.; Jassim, A.H.; Abulqasim, S.A.; Basem, A.; Ogaili, A.A.F.; Al-Haddad, L.A. Leak detection and localization in water distribution systems using advanced feature analysis and an artificial neural network. *Desalination Water Treatment* 2024, 320, 100685. https://doi.org/10.1016/j.dwt.2024.100685
16. Al-Haddad, L.A.; Jaber, A. Applications of machine learning techniques for fault diagnosis of UAVs. In *Proceedings of the CEUR Workshop Proceedings*; 2022; Vol. 3360, pp. 19–25.
17. Al-Haddad, L.A.; Łukaszewicz, A.; Majdi, H.Sh.; Holovatyy, A.; Jaber, A.A.; Al-Karkhi, M.I.; Giernacki, W. Energy consumption and efficiency degradation predictive analysis in unmanned aerial vehicle batteries using deep neural networks. *Advances in Science and Technology Research Journal* 2025, 19, 21–30. https://doi.org/10.12913/22998624/201346
18. Sarow, S.A.; Flayyih, H.A.; Bazerkan, M.; Al-Haddad, L.A.; Al-Sharify, Z.T.; Ogaili, A.A.F. Advancing sustainable renewable energy: XGBoost algorithm for the prediction of water yield in hemispherical solar stills. *Discover Sustainability* 2024, 5, 510. https://doi.org/10.1007/s43621-024-00782-6
19. Al-Haddad, L.A.; Kahachi, H.A.H.; Ur Rehman, H.Z.; Al-Zubaidi, A.A.; Al-Karkhi, M.I.; Al-Oubaidi, B. Advancing sustainability in buildings using an integrated aerodynamic façade: potential of artificial intelligence. *Terra Joule Journal* 2024, 1(1), 1.
20. Al-Karkhi, M.I.; Rzadkowski, G.; Ibraheem, L.; Aqib, M. Anomaly detection in electrical systems using machine learning and statistical analysis. *Terra Joule Journal* 2024, 1(2), 3.
21. Hashim, F.A.; Mohialden, Y.M.; Hussien, N.M. Hybrid feature selection and ensemble classification for climate change indicators: a machine learning approach. *Terra Joule Journal* 2025, 1(2), 8.
22. Mejbel, B.G.; Sarow, S.A.; Al-Sharify, M.T.; Al-Haddad, L.A.; Ogaili, A.A.F.; Al-Sharify, Z.T. A data fusion analysis and random forest learning for enhanced control and failure diagnosis in rotating machinery. *Journal of Failure Analysis and Prevention* 2024, 24, 2979–2989. https://doi.org/10.1007/s11668-024-02075-6
23. Al-Haddad, L.A.; Jaber, A.A.; Mahdi, N.M.; Al-Haddad, S.A.; Al-Karkhi, M.I.; Al-Sharify, Z.T.; Farhan Ogaili, A.A. Protocol for UAV fault diagnosis using signal processing and machine learning. *STAR Protocols* 2024, 5(4), 103351. https://doi.org/10.1016/j.xpro.2024.103351
24. Al-Haddad, A.A.; Al-Haddad, L.A.; Al-Haddad, S.A.; Jaber, A.A.; Khan, Z.H.; Rehman, H.Z.U. Towards dental diagnostic systems: synergizing wavelet transform with generative adversarial networks for enhanced image data fusion. *Computers in Biology and Medicine* 2024, 182, 109241.

https://doi.org/10.1016/j.compbiomed.2024.109241

25. Alawee, W.H.; Al-Haddad, L.A.; Basem, A.; Al-Haddad, A.A. A data augmentation approach to enhance breast cancer detection using generative adversarial and artificial neural networks. *Open Engineering* 2024, 14(1), 20240052. https://doi.org/10.1515/eng-2024-0052
26. Al-Haddad, S.A.; Al-Haddad, L.A.; Jaber, A.A. Environmental engineering solutions for efficient soil classification in southern Syria: a clustering-correlation extreme learning approach. *International Journal of Environmental Science and Technology* 2024, 22, 2177–2190. https://doi.org/10.1007/s13762-024-05784-5
27. Alawee, W.H.; Jaber, A.A.; Omara, Z.M.; Mohammed, S.A.; Dhahad, H.A.; Khan, Z.H.; Al-Haddad, L.A. Optimizing water resources for sustainable desalination: the integration of expert systems and solar energy in experimental applications. *Desalination and Water Treatment* 2024, 320, 100683. https://doi.org/10.1016/j.dwt.2024.100683
28. Al-Haddad, L.A.; Jaber, A.A.; Dhahir, M.K.; Nagim, H.Y.; Algburi, Z.I. Characterization and prediction of femtosecond laser induced tracks in silver-containing zinc phosphate glass. In *Proceedings of the CEUR Workshop Proceedings*; 2024; Vol. 3870, pp. 10–19.
29. Bunyan, S.T.; Khan, Z.H.; Al-Haddad, L.A.; Dhahad, H.A.; Al-Karkhi, M.I.; Ogaili, A.A.F.; Al-Sharify, Z.T. Intelligent thermal condition monitoring for predictive maintenance of gas turbines using machine learning. *Machines* 2025, 13(5), 401. https://doi.org/10.3390/machines13050401
30. Abdulameer, A.G.; Mrah, M.M.; Bazerkan, M.; Al-Haddad, L.A.; Al-Karkhi, M.I. Machine learning-driven power prediction in continuous extrusion of pure titanium for enhanced structural resilience under extreme loading. *Discovery Materials* 2025, 5, 7. https://doi.org/10.1007/s43939-024-00175-6
31. Hussein, R.M.; Hadi, A.S.; Hasan, S.F.; Al-Haddad, L.A.; Harrabi, R.; Flah, A.; Sahib, I.A.A. Hybrid integral sliding mode and fuzzy logic control for omnidirectional robots: modified elephant herding optimization for trajectory tracking. *Scientific Reports* 2025, 15, 35666. https://doi.org/10.1038/s41598-025-19449-x